Environ. Water Eng., 2025, 11(4), 499-508 https://doi.org/10.22034/ewe.2025.501770.1999

EWE

Environment and Water Engineering

Homepage: www.jewe.ir

ISSN: 2476-3683

Investigation of wave characteristics generated by mass landslides and the effect of their arrangement on wave features in a reservoir

Mohammad Bagher Imani[1], Ehsan Delavari[1]✉, Shamsa Basirat[1], and Mohsen Saadat[1]

[1]Department of Civil Engineering, Najafabad Branch, Islamic Azad University, Najafabad, Iran

ARTICLE INFO

Paper Type: Research Paper

Received: 23 January 2025
Revised: 15 February 2025
Accepted: 03 April 2025
Published: 15 May 2025

Keywords
Experimental Investigation
Maximum Wave Height
Rectangular Tank
Sliding Mass

Corresponding author:
E. Delavari
✉ e_delavari@pci.iaun.ac.ir

ABSTRACT

This study experimentally investigates how specific factors, such as the arrangement of concrete cylinders, ramp angle, and the presence or absence of a downstream barrier, influence shock wave characteristics to improve risk prediction accuracy. To do this, three models were considered: two sequential, distant pairs of cylinders (Model 1); two sequential, adjacent pairs of cylinders (Model 2); and four sequential, separate cylinders (Model 3). The concrete cylinders were released into the tank in different models and at three different slopes, either with a downstream barrier or without. The results showed that, when using a downstream barrier, the maximum wave height in models 1, 2, and 3 decreased by 14.5%, 10.5%, and 8.63%, respectively, at three different angles. Comparing results for a particular angle revealed that waves generated by model 3 had higher values in wave height, length, and amplitude among all models. Additionally, the maximum water level fluctuations in Model 3 were 10.1% and 5.4% higher than those in Models 2 and 1, respectively. Increasing the ramp angle in Model 3 raised the wave height by 14.4%.

Highlights

- Effect of downstream barriers on reducing wave height and oscillations.
- Comparative analysis of three sliding mass models in wave generation.
- Identification of the critical model with maximum wave height and length.
- Quantitative assessment of slope angle in amplifying wave characteristics.

How to cite this paper:
Imani, M. B., Delavari, E., Basirat, S., & Saadat, M. (2025). Investigation of wave characteristics generated by mass landslides and the effect of their arrangement on wave features in a reservoir. *Environment and Water Engineering*, *11*(4), 499-508. https://doi.org/10.22034/ewe.2025.501770.1999

1. Introduction

Landslides are one of the major natural phenomena that have long been of significant concern and subject to extensive scientific investigation. In reservoir environments, landslides can cause severe impacts on both the structural integrity and the operational performance of reservoirs. When a landslide occurs, the lateral slopes of the reservoir undergo failure, resulting in the displacement of soil and rock masses of varying sizes and geometries into the impounded water body. These masses may creep slowly, fall freely, or slide along a failure surface. Landslide-induced instabilities reduce the safety of dams, thereby increasing the risk of catastrophic flooding. Flood events pose widespread and serious threats to both human communities and natural resources. Landslides entering reservoirs can generate intense impulse waves within the impoundment, which not only compromise reservoir stability but also trigger disastrous hazards for downstream populations (Rauter et al., 2022).

Field investigations have shown that, depending on the entry depth of the sliding mass relative to the water surface, landslide-generated impulse waves can be categorized into three types: subaerial, submarine, and partially submerged slides (Pilvar et al., 2019). To study such waves, researchers employ a wide range of methodologies, including physical modeling, numerical simulations, and analytical approaches (Yin et al., 2012; Evers et al., 2019; Du et al., 2020). Laboratory-scale investigations have demonstrated that the generation of an impulse wave due to a landslide is a multi-stage and complex process, involving the high-velocity impact of the sliding mass, its deformation and penetration into the

water, flow separation, the formation of a hydrodynamic crater, and ultimately the initiation of the impulse wave itself (Fritz et al., 2003). Studies on the role of landslide deformation in wave generation have revealed that during the early stages, the thickness of the sliding mass decreases approximately linearly with time, while its length increases with the runout distance, resulting in a forward shift of the center of mass (Watts et al., 2003).

In addition, the release velocity of the mass, which is governed by gravitational acceleration on the slope, and the subsequent motion of the slide under water are crucial governing parameters in wave generation (Panizzo et al., 2005; Amini et al., 2022). For subaerial slides, it has been reported that the maximum wave crest amplitude is highly sensitive to the slope angle of the reservoir bed, the impact velocity of the slide, its thickness, kinematics, and geometry (Ataie-Ashtiani & Nik-Khah, 2008). Heller and Hager (2010) further investigated subaerial landslide-generated impulse waves in a prismatic channel by considering Froude similarity and granular slide material. Their experimental framework involved seven governing parameters, including reservoir water depth, impact velocity, slide thickness, slide volume, bulk density, impact angle, and particle size. Their findings indicated that all parameters, except for particle size (which showed negligible influence), significantly affected wave generation. Heller et al. (2011) studied the effect of slide geometry on wave height, amplitude, period, and propagation speed using small-scale physical models. Their results highlighted that the discrepancy between two-dimensional and three-dimensional wave heights was approximately 20% at a distance of five times the water depth from the impact zone, with the difference increasing at greater distances. Furthermore, the accuracy of experimental data decreased as the slope angle increased, and both 2D and 3D models at steep angles were found to poorly simulate real-world conditions, while significantly raising experimental costs. Huang et al. (2017) concentrated on shallow reservoirs and reported that increasing slide impact distance led to higher pressures, whereas increasing slope inclination initially lowered the peak pressure before causing it to rise again.

Kim et al. (2020) numerically investigated tsunami hazards generated by landslides and solid body impacts in the Gulf of Mexico. Their results showed that numerical models generally yielded acceptable error levels in validation tests, except in near-field conditions close to the wave generation zone. Based on their findings, recommendations were made for dam design and redesign in that region. Romano et al. (2020) examined wave generation due to a sliding body on an inclined plane using both numerical and experimental approaches, reporting excellent agreement with analytical predictions. They showed that upon impact, elliptical vortices initially formed, gradually evolving into circular vortices before dissipating. Basirat et al. (2022) applied the finite volume method with overlapping grids to numerically investigate impulse wave generation by a sliding block. Their results indicated that increasing slide density from 2100 to 2900 kg/m³ and the nondimensional release height of the slide led to increases in the single-wave height by 24% and 20%, respectively. Similarly, Huang et al. (2022) simulated landslide-generated tsunamis in reservoir environments, emphasizing that such hazards cannot be neglected in dam safety assessments. Kafle et al. (2023) examined the dynamics of landslide-generated tsunamis, focusing on the impact of sediment concentration in the released mass. Their simulations revealed that high-concentration mass flows create stronger tsunamis that propagate faster, greatly increasing dam failure risks. Dignan et al. (2023) used probabilistic simulations to assess landslide-generated tsunami hazards in Indonesia's Makassar Strait, predicting maximum wave amplitudes of up to 10 m along the eastern shoreline and 50 m along the western coast. Their models provided high predictive accuracy, with discrepancies between simulated and observed values generally less than 0.7 m. Rubin et al. (2023) analyzed landslide-generated impulse waves through 18 laboratory tests in V-shaped channels, reporting that the resulting waveforms were weakly nonlinear oscillatory waves, consisting of a leading periodic wave with positive amplitude followed by smaller oscillatory waves. They also proposed a regression model for estimating wave parameters. More recently, Xingchen et al. (2024) performed large-scale physical experiments on partially submerged landslides with low Froude numbers, deriving predictive formulas for wave height and amplitude with accuracies ranging between 56% and 89.5%. Darvenne et al. (2024) used a two-dimensional experimental model to assess how granular slide flows influence impulse wave generation and introduced a new Froude number for better characterization of the phenomenon. Ma et al. (2024) conducted probabilistic analyses of impulse waves in mountain reservoirs by coupling SPH-SWEs with an LSTM neural network, demonstrating that slide velocity is more critical than slide volume in determining wave height. Their results showed that in 84% of cases, the run-up height ranged from 5.7 m to 9.5 m.

Due to slope failures along reservoir banks, large impulse waves can form within the impounded lake. These waves may cause significant damage to shoreline facilities, dam structures, nearby hydraulic infrastructures, and upstream and downstream residential and agricultural areas. Therefore, understanding and predicting the characteristics of landslide-generated impulse waves in reservoirs requires careful analysis of the key parameters influencing their formation, movement, and distribution within the reservoir. Previous research has primarily focused on impulse waves caused by subaerial slides entering the reservoir's free surface, while fewer studies have examined different sliding mass geometries, various slope angles, or the presence of barriers within the impoundment. As a result, this experimental study investigates wave heights caused by the impact of cylindrical sliding masses under different slope conditions, with and without barriers in the reservoir model.

2. Materials and Methods

entire experimental setup, including the wave tank, sliding slope, and rigid sliding mass, was designed and The constructed by the authors from scratch to physically model the effects of mass landslides impacting a reservoir. The experiments were conducted in a rectangular flume measuring 10 m in length, 4 m in width, and 1.2 m in depth. The cross-sectional dimensions of the flume were selected to minimize scale effects (Fritz et al., 2004). The main frame of the flume was made of steel to handle both static and dynamic loads, while its sidewalls consisted of laminated double-glass panels,

and the flume bed remained horizontal (0° slope). To accurately observe the entry of the sliding mass into the water and the resulting impulse waves, and to eliminate light reflections during image capture, one side of the glass flume was covered with a white fabric screen. Additionally, two high-resolution cameras were installed on the remaining sides to record the experimental events (Daneshfaraz et al., 2021; Karami Moghadam et al., 2020). Figure 1 illustrates the details of the experimental flume used in the present study, along with the video recording setup and camera arrangement.

Fig. 1 The schematic view of the rectangular tank, along with the replacement of laboratory equipment

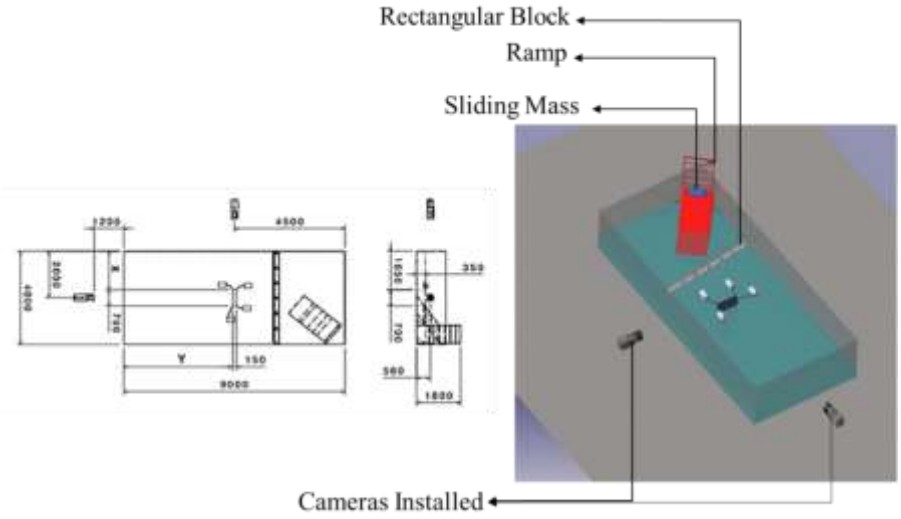

Based on the experimental program proposed by Panizzo et al. (2005) and the findings of that study, a sliding slope was installed at one corner of the flume to release sliding masses into the reservoir. The sliding plane measured 2.0 m in length and 1.0 m in width, and was tested at three heights: 0.85 m, 1.05 m, and 1.25 m. These heights corresponded to slope angles of 23.03°, 27.7°, and 32.01°, respectively. The water depth in the reservoir was kept at 0.55 m for all experiments. While most previous studies on landslide impacts into reservoirs have used block shapes such as cuboids or square prisms (Panizzo et al., 2005; Ataie-Ashtiani & Nik-Khah, 2008; Huang et al., 2017), this study used cylindrical concrete blocks as sliding masses. The cylindrical blocks were placed at the top of the slope with zero initial velocity, then released to accelerate under gravity and impact the water body. In addition, a rectangular barrier with a height of 25 cm and a width of 37 cm was installed 1.5 m from the slope toe to examine the effect of an internal barrier. The blocks were arranged side by side across the entire 4 m width of the flume (Fig. 2). High-speed cameras capable of recording 30 frames per second were used to capture the block entry and subsequent impulse wave generation. Based on trial-and-error testing, a 6 m observation length was found sufficient to fully record the experimental events, and thus the camera system was adjusted to cover this section of the flume. Water surface profiles were recorded at distances of 1.5 m, 3.0 m, 4.5 m, and 6.0 m from the sliding slope at successive time intervals (De Carvalho & Antunes do Carmo, 2007). For each experimental run, a 5-second sequence (20 frames) was recorded (Bagherzadeh and Mohammadi, 2025). The image data were processed using MATLAB and its image-processing toolbox to extract quantitative water surface elevations. Fig. 2 and Table 1 present the specifications of the three sliding block models employed in this study. For consistent comparison and clearer interpretation of results, the free-surface elevations of all models were normalized around 0.25 m. Accordingly, the initial reservoir depth of 0.55 m was reduced by 0.30 m, and the resulting water surface oscillations were reported in centimeters (Owtad et al., 2024).

Fig 2. Three different models of cylinders' arrangement and fall geometry

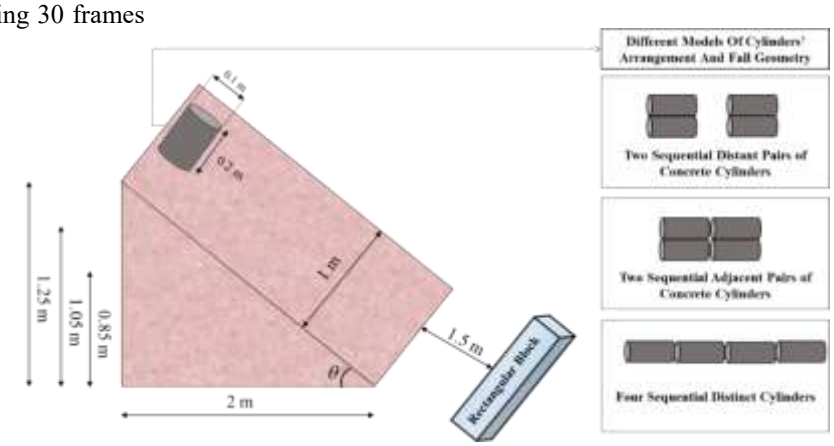

Table 1 Characteristics of the three models used in the research

Model	Fall geometry	Vertical distance from the water surface (m)	Density of concrete (kg/m^3)	Angle of the ramp (degrees)	Water depth (m)
Model 1	two sequential distant pairs of concrete cylinders	0.85, 1.05, and 1.25	2419	23.03, 27.7, and 32.01	0.55
Model 2	two sequential adjacent pairs of concrete cylinders				
Model 3	Four sequential, distinct cylinders				

In this study, the first stage of investigation focused on assessing the effect of a barrier placed downstream of the sliding slope, followed by examining the arrangement of sliding block models released at different slope angles. The experimental program was carried out in three stages. The first stage studied how the barrier affected wave characteristics caused by sliding masses. A barrier composed of rectangular blocks, each 37 cm wide and placed side by side across the entire flume width with a height of 25 cm, was installed at a distance of 1.5 m from the toe of the inclined plane. The second stage explored how the geometry and arrangement of the sliding mass influenced wave generation. To investigate the influence of slide arrangement and configuration, three models of mass failure were considered: four cylinders released sequentially with spacing (M1), four cylinders released sequentially without spacing (M2), and four cylinders released simultaneously in parallel (M3). The third stage evaluated how the slope angle impacted free-surface variations and wave formation resulting from landslide impacts. The models were released into the reservoir at three slope angles of 23.03°, 27.7°, and 32.01°. In all experiments, the bulk density of the sliding masses and the reservoir depth were kept constant (water depth of 0.55 m).

3. Results and Discussion

3.1 The effect of the barrier

In open-channel flows, variations in velocity or flow depth over time or space are called waves. In this study, experiments were conducted to examine how barriers (wave breakers) placed downstream of the sliding slope affect wave characteristics. For this purpose, three sliding mass models were released from the ramp at three different inclination angles (Table 1) into a rectangular reservoir with a constant water depth of 0.55 m. The barriers were made of rectangular blocks measuring 25×37 cm, arranged across the entire width of the flume. The barrier system was positioned 1.5 m downstream of the slope toe, where the cylindrical sliding blocks were released (Fig. 2).

The effects of these barriers on the maximum wave heights are illustrated graphically in Fig. 3 for all three sliding models and slope conditions. The results demonstrated that the presence of barriers significantly reduced wave characteristics, including wave height and wavelength. On average, across all three slopes, the maximum wave height was reduced by 14% for Model 1, by 10.5% for Model 2, and by 8.63% for Model 3. A detailed summary of the results for all slope conditions and models is provided in Table 2. Without barriers, Model 3 produced the largest maximum wave height, reaching 34.98 cm. This observation can be explained by the fact that increasing the slope angle enhances the gravitational force acting downslope, which accelerates the sliding mass and consequently increases the wave parameters produced. Conversely, when barriers are present, steeper slopes increase the impact force between the sliding mass and the barrier. This interaction dissipates more energy during collision, thus reducing the landslide's contribution to wave generation in the reservoir. The reduction in wave height and amplitude observed in this study due to downstream barriers is consistent with previous experimental findings on submerged breakwaters. Dattatri et al. (1978) showed that breakwaters dissipate wave energy by inducing turbulence and modifying flow patterns, resulting in lower wave heights downstream. Similarly, Kubowicz-Grajewska (2015) reported that submerged structures reduce wave-induced morphodynamic changes by attenuating wave energy and controlling flow propagation. These results support our observations that barriers effectively mitigate landslide-generated waves, with greater slope angles enhancing barrier performance due to higher slide velocities and increased energy transfer. The combination of barrier placement and slope considerations is critical for optimizing wave reduction in reservoirs. Overall, the findings indicate that lower slopes weaken the barrier's effectiveness, while higher slopes improve its ability to mitigate wave characteristics. In other words, barriers become more effective at reducing the impact of landslide-generated waves as slope angles become steeper.

3.2 Effect of geometry and arrangement of concrete cylinders

Experimental observations revealed that the arrangement and configuration of the slides had a significant effect on the overall sliding process. In model M1, which consisted of four cylinders with spacing, the masses descended sequentially in an orderly manner. During this process, the first cylinder hit the second, transferring some of its energy and causing the second cylinder to slide into the reservoir at a higher speed. In contrast, in model M2, which involved four cylinders released sequentially without spacing, the masses moved more as a single unit and showed greater stability during sliding because the spacing was eliminated. In model M3, with four cylinders released simultaneously in parallel, the masses uniformly descended side by side.

Fig. 3 Comparing the results of the water level profile in the presence and absence of the breakwater, a) Model 1, b) Model 2, and c) Model 3

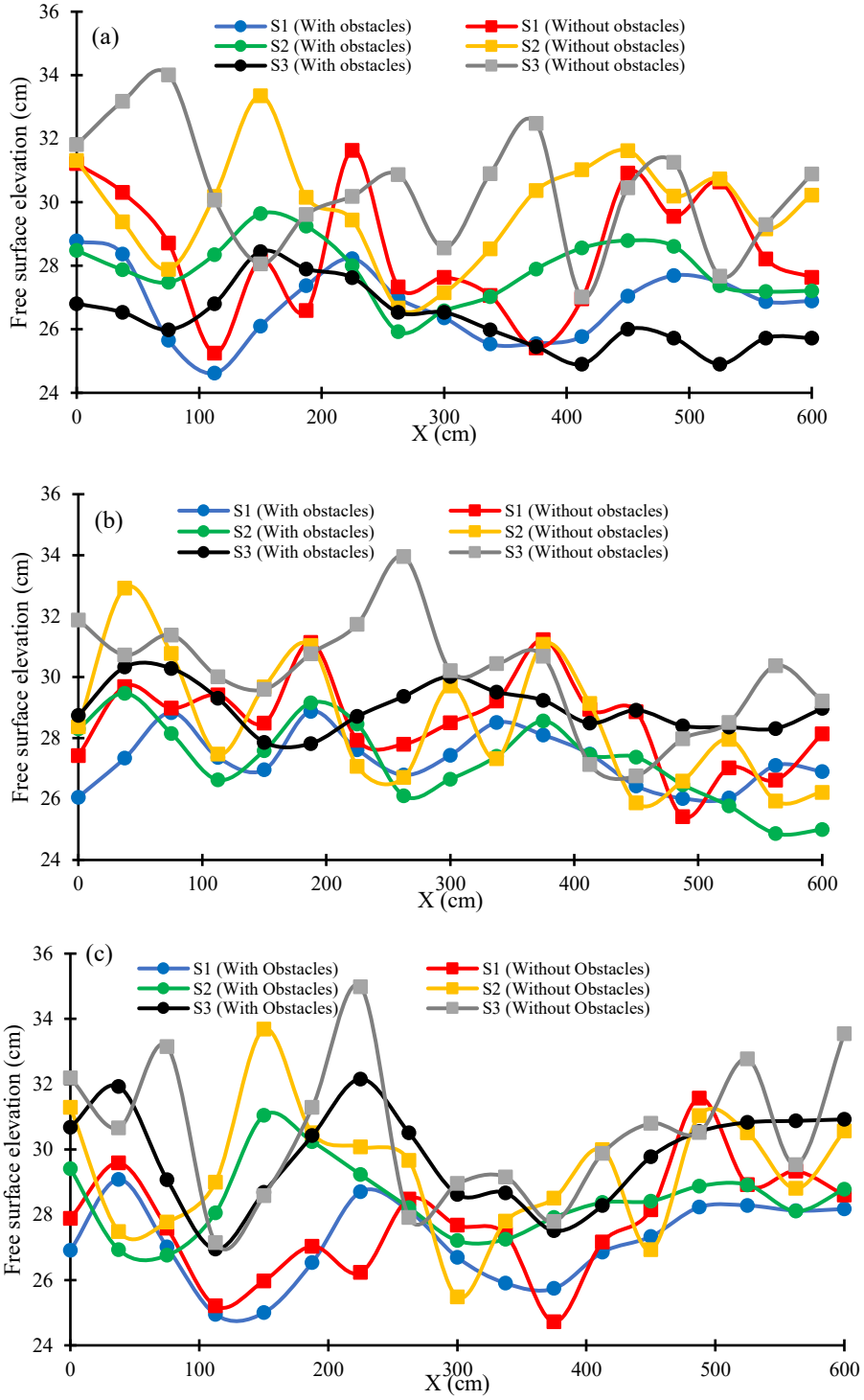

Table 2 Maximum values of wave height reduction in the presence of a breakwater (%)

Model	S_1	S_2	S_3	Average
Model 1	9.93	12.52	19.57	14.01
Model 2	8.13	11.72	11.95	10.60
Model 3	8.58	8.52	8.78	8.63

The wave patterns generated by these three models exhibited distinct features. Waves in model M2 were more stable and symmetric compared to those in models M1 and M3, while models M1 and M3 produced more turbulence and irregularities. Specifically, in model M1, the sequential impacts during sliding generated waves that were relatively low in height and had larger wavelengths compared to model M2. Conversely, in model M3, the simultaneous effect of the four cylinders generated waves that were taller and covered a

larger surface area. These laboratory results highlight the important influence of slide arrangement and configuration on the stability and behavior of mass failures, as well as the waves they generate. Fig. 4 presents the water surface profiles along the reservoir for all three models during the first 1–5 seconds of sliding. According to Fig. 4, for a given slope angle, model M3 consistently exhibited higher wave characteristics, including height, length, and amplitude, compared to models M1 and M2. Among the three, model M3 was identified as the most critical sliding condition, with the highest wave parameters. For example, in model M3, a maximum wave height of 29.94 cm was recorded at t=4 s for a slope of 23.03°. For slopes of 27.7° and 32.01°, the maximum wave heights were 31.04 cm and 32.51 cm, observed at t = 5 s and t=3 s, respectively.

Fig. 4 The diagram of the water level profile versus the length of the tank: a) T=1 S, b) T=2 S, c) T=3 S, d) T=4 S, e) T=5 S, of the falling process

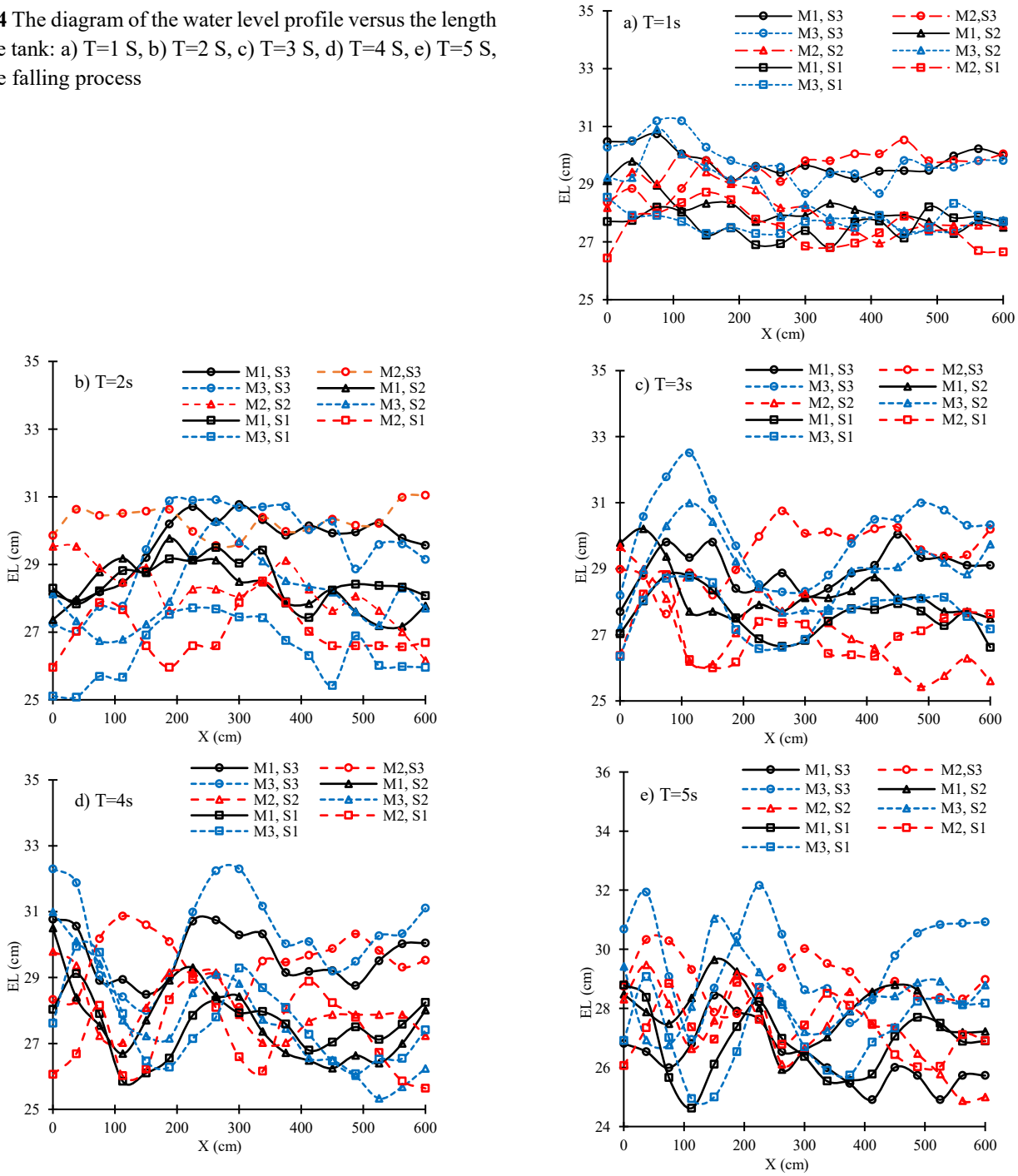

The relative differences in maximum wave heights between model M3 and model M2 for the steepest and gentlest slopes were 4.5 and 3.3%, respectively, while for model M1, they were 5.3 and 1.5%, respectively. Although the differences among the models were relatively small, the results consistently ranked model M3 as the most critical, followed by model M1 and then model M2, in terms of sliding scenarios. A closer comparison of models M1 and M2 also indicated that model M1 produced more turbulence and irregularities on the water surface during sliding. The temporal analysis of recorded data revealed that maximum wave heights occurred at different times: at t=3 s for model M3, at t=2 s for model

M2, and at t=4 s for model M1. Additionally, the results confirmed that increasing the slope angle for any given model increased wave characteristics such as wave height, wave steepness, and turbulence in the reservoir.

Figure 5 shows the changes in wave height within the reservoir during the 1–5 second interval for different measurement points. As shown in Fig. 5, it is clear that the oscillatory response of the water surface caused by the sliding models depends on the shape of the sliding mass and the angle of the sliding surface, resulting in different outcomes at various reservoir locations. In all models, placing a barrier 1.5 m from the sliding slope effectively controlled the waves in this area by reducing water surface oscillations and creating a more consistent wave pattern across the three models. Essentially, the barrier acted as a breakwater, damping fluctuations in this zone.

Fig. 5 The diagram of the wave height changes over 5 seconds: a) S_1=23°, x=1.5 m, b) S_1=23°, x=3 m, c) S_1=23°, x=4.5 m, d) S_1=23°, x=6 m, e) S_2=27.7°, x=1.5 m, f) S_2=27.7°, x=3 m, g) S_2=27.7°, x=4.5 m, h) S_2=27.7°, x=6 m, i) S_3=32°, x=1.5 m, j)S_3=32°, x=3 m, k) S_3=32°, x=4.5 m, l) S_3=32°, x=6 m

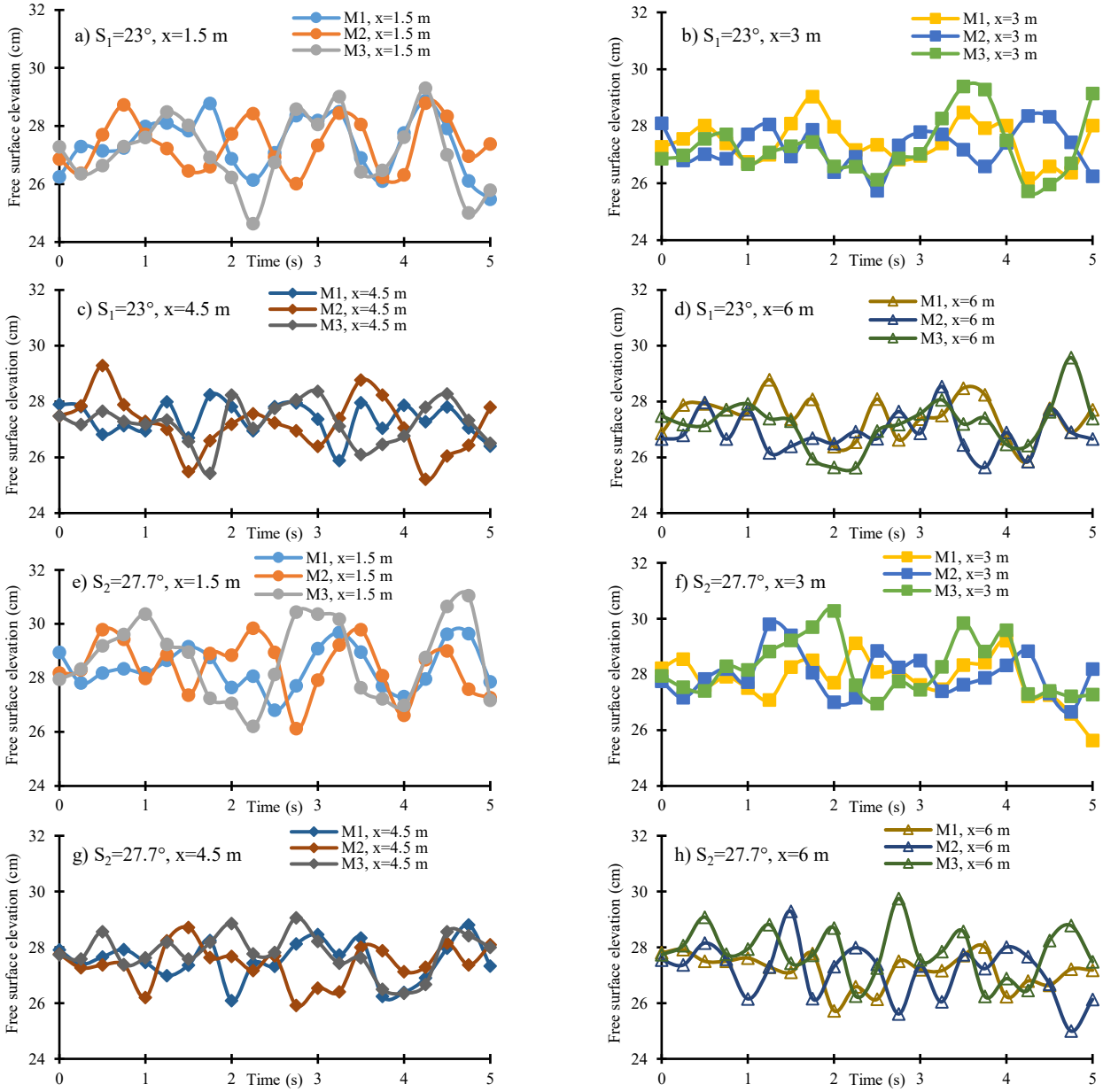

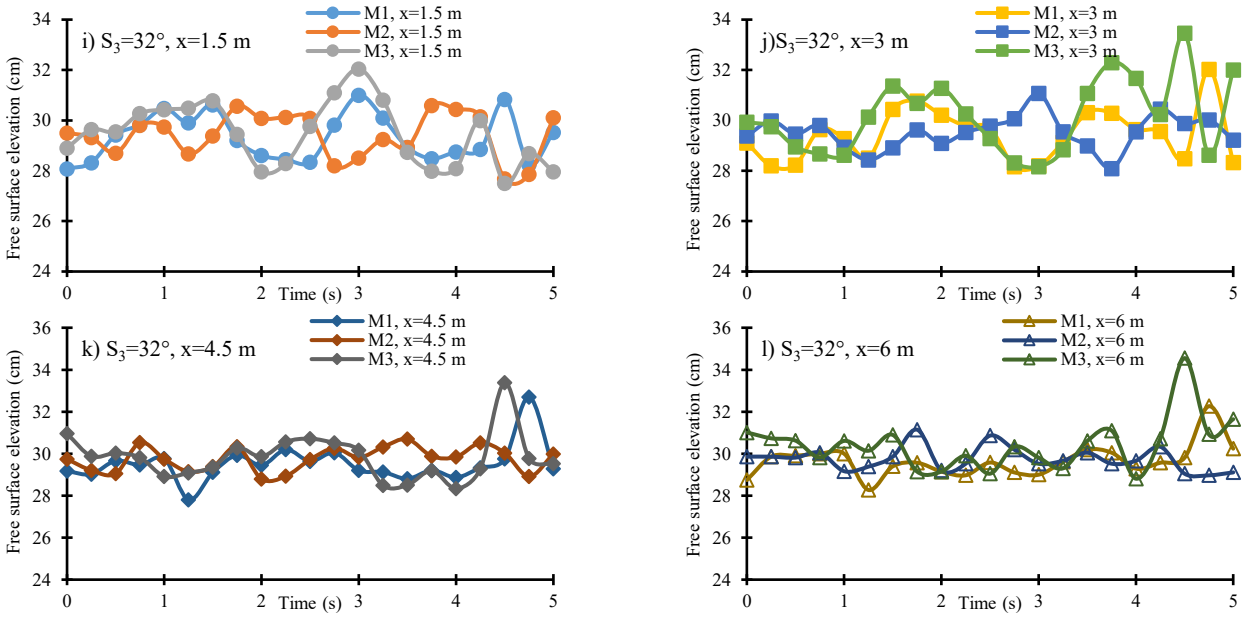

The analysis of sliding geometries revealed that, for a constant slope and location, the parallel arrangement of cylindrical masses (Model 3) generated the highest wave height. Furthermore, laboratory observations indicated that this model, along with Model 1 (four cylinders released sequentially with spacing), produced waves with high irregularity and unpredictable oscillation patterns. In contrast, Model 2 exhibited more uniform oscillations with relatively consistent frequencies, while Models 1 and 3 displayed irregular and chaotic wave responses. Table 3 presents the overall results of the experiments for all sliding mass configurations at the three tested slope angles. It was observed that in Model 2, wave oscillations with relatively low heights were concentrated within the first 1.5 m, while in the other models, the maximum oscillations occurred downstream of the barrier. Among the tested cases, Model 3 produced the most critical condition, with a maximum wave height of 34.55 cm at 4.5 s and 6 m from the source under the steepest slope. For the mildest slope, the same model generated a wave height of 29.57 cm at 6 m from the ramp. Comparative analysis showed that, under the steepest slope, the oscillation height in Model 3 was 10.1% greater than in Model 2 and 5.4% greater than in Model 1. Overall, the results confirmed that increasing the slope angle led to higher wave parameters. A comparison of slopes across the three models further indicated that wave height increased by 11.2% in Model 1, 5.7% in Model 2, and 14.4% in Model 3 as the slope angle increased. These findings are consistent with the experimental observations of Owtad et al. (2024), who reported that the arrangement and parallel placement of sliding masses significantly influence wave height and energy in rectangular water reservoirs.

Table 3 The results of maximum water level fluctuations for three models

	Ramp angle (slope)		
Model	S_1=23°	S_2=27°	S_3=32°
Model 1	X=3 m t=1.75 s max=29.04 cm min=26.16 cm	X=1.5 m t=3.25 s max=29.68 cm min=26.8 cm	X=4.5 m t=4.75 s max=32.69 cm min=27.8 cm
Model 2	X=4.5 m t=0.5 s max=29.29 cm min=25.21 cm	X=1.5 m t=2.25 s max=29.83 cm min=26.11 cm	X=6 m t=1.75 s max=31.14 cm min=28.97 cm
Model 3	X=6 m t=4.75 s max=27.83 cm min=25.63 cm	X=1.5 m t=4.75 s max=31.04 cm min=26.19 cm	X=6 m t=4.5 s max=34.55 cm min=28.81 cm

4. Conclusion

In the present study, laboratory experiments were conducted to investigate the oscillations and waves generated by landslides and mass failures into a reservoir. The experiments were performed for three sliding mass models and three slope angles under two conditions: with and without a barrier placed downstream of the sliding slope. The overall findings are summarized as follows:

1. Laboratory observations indicated that the placement of a barrier 1.5 m downstream of the sliding slope reduced water surface oscillations within the reservoir and mitigated the formation of irregular waves. Comparatively, the presence of the barrier led to a reduction in maximum wave height by an average of 14%, 10.5%, and 8.63% for Models 1, 2, and 3, respectively, across the three slope angles.

2. For a fixed slope, comparison along the reservoir length indicated that Model 3 exhibited the largest wave characteristics, including wave height, length, and amplitude. Specifically, for minimum and maximum slopes, the maximum wave heights recorded for Model 3 were 29.94 cm and 32.51 cm, respectively. The percentage difference in maximum wave height of Model 3 relative to Model 2 was 4.5% and 3.3% for maximum and minimum slopes, respectively.

3. Analysis of wave height versus time revealed that for the steepest slope, Model 3 generated a wave of 34.55 cm at 6 m from the ramp. The peak wave height of Model 3 was 10.1% higher than Model 2 and 5.4% higher than Model 1. Examining the sliding geometry revealed that, for a fixed slope and position, the parallel release of cylindrical masses (Model 3) produced the highest wave height.

4. Increasing the slope angle enhances the wave characteristics generated within the reservoir. Comparing slopes revealed that increasing the slope angle increased wave height by 11.2% for Model 1, 5.7% for Model 2, and 14.4% for Model 3.

It is recommended that future research explore barrier placement at different distances and the simultaneous use of multiple barrier series in laboratory tests to compare with the present findings.

Statements and Declarations

Data availability

The data supporting the findings of this study are available from the corresponding author upon reasonable request via email: e_delavari@pci.iaun.ac.ir.

Conflicts of interest

The authors of this paper declared no conflict of interest regarding the authorship or publication of this paper.

Author contribution

All authors contributed to the preparation of the manuscript, the analysis and interpretation of data, and the critical revision of the article content.

AI Use Declaration

During the preparation of this work, the author(s) used ChatGPT to improve some sentences. The authors have thoroughly reviewed and revised the content as necessary and assumed full responsibility for the final manuscript.

References

Ataie-Ashtiani, B., & Nik-Khah, A. (2008). Impulsive waves caused by subaerial landslides. *Environmental Fluid Mechanics*, *8*, 263-280. https://doi.org/10.1007/s10652-008-9074-7

Ataie-Ashtiani, B., & Yavari-Ramshe, S. (2011). Numerical simulation of wave generated by landslide incidents in dam reservoirs. *Landslides*, *8*, 417-432. https://doi.org/10.1007/s10346-011-0258-8

Amini, A., Bahrami, J., & Miraki, A. (2022). Effects of dam break on downstream dam and lands using GIS and HEC-RAS: A decision basis for the safe operation of two successive dams. *International Journal of River Basin Management,* *20*(4), 487–498. https://doi.org/10.1080/15715124.2021.1901728

Basirat, S., Mokhtarzadeh, G., Bazargan, J., & Delavari, E. (2022). Numerical Investigation of Wave Production due to Mass Slip Using Finite Volume Method and Overset Mesh. *Water Resources Engineering*, *15*(54), 43-56. https://doi.org/10.30495/wej.2022.27135.2291 (In Persian).

Karami Moghadam, M., Amini, A., & Keshavarzi, A. (2020). Intake design attributes and submerged vanes effects on sedimentation and shear stress. *Water and Environment Journal,* *34*(3), 374–380. https://doi.org/10.1111/wej.12471

Bagherzadeh, M., & Mohammadi, M. (2025). Impact of Gabion Sill on Scouring Depth Downstream Grade Control Structures. *Results in Engineering*, 105717. https://doi.org/10.1016/j.rineng.2025.105717 (Article In Press)

Du, J., Yin, K., Glade, T., Woldai, T., Chai, B., Xiao, L., & Wang, Y. (2020). Probabilistic hazard analysis of impulse waves generated by multiple subaerial landslides and its application to Wu Gorge in Three Gorges Reservoir, China. Engineering Geology, 276, 105773. https://doi.org/10.1016/j.enggeo.2020.105773

Dignan, J., Hayward, M. W., Salmanidou, D., Heidarzadeh, M., & Guillas, S. (2023). Probabilistic landslide tsunami estimation in the Makassar Strait, Indonesia, using statistical emulation. *Earth and Space Science*, *10*(8), e2023EA002951. https://doi.org/10.1029/2023EA002951

De Carvalho, R. F., & Antunes do Carmo, J. S. (2007). Landslides into reservoirs and their impacts on banks. *Environmental Fluid Mechanics*, *7*, 481-493. https://doi.org/10.1007/s10652-007-9039-2

Daneshfaraz, R., Bagherzadeh, M., Ghaderi, A., Di Francesco, S., & Asl, M. M. (2021). Experimental investigation of gabion inclined drops as a sustainable solution for hydraulic energy loss. *Ain Shams Engineering Journal*, *12*(4), 3451-3459. https://doi.org/10.1016/j.asej.2021.03.013

Darvenne, A., Viroulet, S., & Lacaze, L. (2024). Physical model of landslide-generated impulse waves: Experimental investigation of the wave-granular flow coupling. *Journal of Geophysical Research: Oceans*, *129*(9), e2024JC021145. https://doi.org/10.1029/2024JC021145

Dattatri, J., Raman, H., & Shankar, N. J. (1978). Performance characteristics of submerged breakwaters. *Coastal*

Engineering 1978 (pp. 2153-2171). https://doi.org/10.1061/9780872621909.132

Evers, F. M., Hager, W. H., & Boes, R. M. (2019). Spatial impulse wave generation and propagation. *Journal of Waterway, Port, Coastal, and Ocean Engineering*, *145*(3), 04019011. https://doi.org/10.1061/(ASCE)WW.1943-5460.0000514

Fritz, H. M., Hager, W. H., & Minor, H. E. (2003). Landslide generated impulse waves. *Experiments in Fluids*, 35, 505-519. https://doi.org/10.1007/s00348-003-0659-0

Fritz, H. M., Hager, W. H., & Minor, H. E. (2004). Near field characteristics of landslide generated impulse waves. *Journal of waterway, port, coastal, and ocean engineering*, *130*(6), 287-302. https://doi.org/10.1061/(ASCE)0733-950X(2004)130:6(287)

Heller, V., Hager, W. H., & Minor, H. E. (2010). Landslide generated impulse waves in reservoirs: Basics and computation. *VAW-Mitteilungen*, *211*. https://doi.org/10.3929/ethz-b-000157446

Heller, V., Moalemi, M., Kinnear, R. D., & Adams, R. A. (2011). Geometrical effects on landslide-generated tsunamis. *Journal of waterway, port, coastal, and ocean engineering*, *138*(4), 286-298. https://doi.org/10.1061/(ASCE)WW.1943-5460.0000130

Huang, B., Wang, S. C., & Zhao, Y. B. (2017). Impulse waves in reservoirs generated by landslides into shallow water. *Coastal Engineering*, 123, 52-61. https://doi.org/10.1016/j.coastaleng.2017.03.003

Huang, T., Zhang, H., & Shi, Y. (2022). Numerical simulation of landslide-generated tsunamis in lakes: A case study of the Xiluodu Reservoir. *Science China Earth Sciences*, 1-15. https://doi.org/10.1007/s11430-022-9989-1

Kafle, J., Dangol, B. R., Tiwari, C. N., & Kattel, P. (2023). Dynamics of landslide-generated tsunamis and their dependence on the particle concentration of initial release mass. *European Journal of Mechanics-B/Fluids*, *97*, 146-161. https://doi.org/10.1016/j.euromechflu.2022.10.003

Kim, G. B., Cheng, W., Sunny, R. C., Horrillo, J. J., McFall, B. C., Mohammed, F., & Kowalik, Z. (2020). Three dimensional landslide generated tsunamis: Numerical and physical model comparisons. *Landslides*, 17, 1145-1161. https://doi.org/10.1007/s10346-019-01308-2

Kubowicz-Grajewska, A. (2015). Morpholithodynamical changes of the beach and the nearshore zone under the impact of submerged breakwaters–a case study (Orłowo Cliff, the Southern Baltic). *Oceanologia*, *57*(2), 144-158. https://doi.org/10.1016/j.oceano.2015.01.002

Ma, H., Wang, H., Shi, H., Xu, W., Hou, J., Wu, W., & Xie, W. C. (2024). Probabilistic landslide-generated impulse waves estimation in mountain reservoirs, a case study. *Bulletin of Engineering Geology and the Environment*, *83*(12), 494. https://doi.org/10.1007/s10064-024-04003-2

Owtad, R., Basirat, S., Delavari, E., hosseini, M., & Hojaji Najafabadi, M. (2024). Experimental study of waves created by sliding masses in a rectangular water reservoir. *Water Resources Engineering*, *17*(62), 16-28. https://doi.org/10.30495/wej.2024.32271.2395 (In Persian).

Panizzo, A., De Girolamo, P., & Petaccia, A. (2005). Forecasting impulse waves generated by subaerial landslides. *Journal of Geophysical Research: Oceans*, *110*(C12). https://doi.org/10.1029/2004JC002778

Pilvar, M., Pouraghniaei, M. J., & Shakibaeinia, A. (2019). Two-dimensional sub-aerial, submerged, and transitional granular slides. *Physics of Fluids*, *31*(11). https://doi.org/10.1063/1.5121881

Romano, A. (2020). Physical and numerical modeling of landslide-generated tsunamis: A review. *Geophysics and Ocean Waves Studies*.

Rauter, M., Viroulet, S., Gylfadóttir, S. S., Fellin, W., & Løvholt, F. (2022). Granular porous landslide tsunami modelling–the 2014 Lake Askja flank collapse. *Nature communications*, *13*(1), 678. https://doi.org/10.1063/1.5121881

Rubin, W., Wang, Y., Wan, J., Xu, W., Yang, Y., & Wang, H. (2023). Propagation Mechanism of Deep-Water Impulse Waves Generated by Landslides in V-Shaped River Channels of Mountain Valleys: Physical Model of Regular Rigid Block. *Geofluids (Online)*, *2023*. https://doi.org/10.1155/2023/1743305

Yin, K. L., Liu, Y. L., Wang, Y., & Jiang, Z. B. (2012). Physical model experiments of landslide-induced surge in Three Gorges Reservoir. *Earth Science/Diqiu Kexue*, *37*(5), (in Chinese).

Watts, P., Grilli, S. T., Kirby, J. T., Fryer, G. J., & Tappin, D. R. (2003). Landslide tsunami case studies using a Boussinesq model and a fully nonlinear tsunami generation model. *Natural hazards and earth system sciences*, *3*(5), 391-402.

Xingchen, D., Bolin, H., Qiuwang, L., Shulou, C., Yang, L., & Guoqiang, Y. (2024). Prediction of impulse waves generated by partially submerged landslides with a low Froude number based on prototype physical experiments. *Physics of Fluids*, *36*(10). https://doi.org/10.1063/5.0233925